sciendo

Slovak Journal of Civil Engineering

Vol. 32, 2024, No. 3, 33 – 40
DOI: 10.2478/sjce-2024-0017

SETTLEMENT ANALYSIS OF THE NIVY TOWER IN BRATISLAVA BY THE FINITE ELEMENT METHOD

Juraj CHALMOVSKÝ[1*], Jan ČERVENKA[1], Ján DOBROVOLSKÝ[2], Václav RAČANSKÝ[3]

Abstract

A settlement analysis of a new high-rise building, the Nivy Tower, in Bratislava, Slovakia, is presented in this paper. A 3D finite element model was prepared. A non-linear elasto-plastic material model with double hardening and increased stiffness in a small-to-very-small strain range was adopted for the Tertiary (Neogene) subsoils. Due to the lack of an appropriate in-situ test, the results from a 1D compression test were used for the calibration of the soil input parameters. However, the results from these tests, especially in the primary loading, are often biased due to the effects of soil disturbance during the preparation of the sample. Therefore, a different procedure has been proposed, in which the stiffness parameters were obtained from unloading-reloading branches of 1D compression tests. It could be concluded that the predicted and measured settlements are in a reasonable match for all the points measured. The computed distributions of the vertical displacements and those measured by sliding micrometres show greater differences from a depth of twenty meters beneath the foundation slab.

Address

[1] Brno University of Technology, Faculty of Civil Engineering, Institute of Geotechnics, Czech Republic
[2] Keller špeciálne zakladanie, spol. s.r.o., Slovakia
[3] Keller Grundbau GmbH., Austria

[*] ***Corresponding author:*** xschalmovskyj@vutbr.cz

Key words

- Foundation slab,
- Jet-grouting,
- Finite element method,
- Soil stiffness,
- Settlement.

1 INTRODUCTION

High-rise structures are an integral part of large cities because of their efficient use of the space available. The building analysed in this paper is situated in a new complex called "New Nivy" in Bratislava, Slovakia, near the Danube river. The high-rise has 32 upper floors and a total height of 125 m. The building also includes a smaller vestibule with 4 upper floors. The high-rise construction was completed in 2020.

A settlement analysis using a 3D finite element model is presented in this paper. A significant amount of 1D compression tests were available, which allowed for the direct determination of a part of the input parameters for the governing soil type. The settlement prediction is classified as type C according to Lambe (1973), which means that the prediction was made after the event, but the available monitoring results did not affect the prediction (the comparison with the measurements was made after the calculations were completed).

The finite element method has been used for high-rise settlement analyses by various authors. *Katzenbach, Schmitt (2004)* presented the finite element simulation of a high-rise in Germany using a double-yield constitutive model with cap hardening. *Sales (2010)* used a combination of a finite element and boundary analysis to predict settlements of both near-surface piled rafts and piled rafts situated in deep excavations. *Poulos (2023)* analysed an interaction of multiple high-rise buildings using a simplified 2D axi-symmetric finite element model. *Ganal, Reul (2023)* utilized a visco-hypoplastic material model for a time-dependent 3D analysis of the raft foundation of a high-rise building in Germany.

An interesting aspect of the Nivy Tower is that it is situated asymmetrically in a much bigger deep excavation with its one side close to the retaining structure. A full 3D model, including the high-rise foundation, retaining structure, and soil massif unaffected by the excavation (with the original ground level) was therefore prepared. Furthermore, in addition to the geodetical levelling at various points of the construction, sliding micrometres were installed in the boreholes under the foundation slab. This provided a unique opportunity to evaluate the accuracy of the computational model not only based on the surface settlements but also based on the vertical distributions of the displacements.

Nivy Tower is a part of a large administrative and commercial development project with overall dimensions of 350 x 175 m on the location of the former central bus station in Bratislava. A high-rise tower with footprint dimensions of 53 x 26 m is founded on a base slab with a thickness of 2.3 m. The characteristic foundation pressure reaches up to 600 kPa. The standard design practice would recommend a heavy piling solution for such boundary conditions. However, there are many references proving that a well-designed soil improvement solution may work equally well and can fulfill the design criteria as requested by structural engineers. As examples with relevance to our case, Florido Tower in Vienna, Austria, can be mentioned as it is located in similar geotechnical conditions of the Vienna Basin. This tower, with a 110 m height and a foundation pressure of up to 400 kPa, was founded on a gravel layer, which was improved and homogenized by a vibro compaction technique. Another relevant example is the Olivia Star in Gdansk, Poland. It is a 156 m tall building founded on jet grouted (JG) columns with a diameter of 1.8 m and lengths between 5 to 13 m and thus using a similar ground improvement scheme as in our case. More details to both references can be found in *Topolnicki (2019)*. The ground improvement scheme for the Nivy Tower uses jet grouting columns of ϕ2.0m with a length from 9 to 18 m. The main contribution of this ground improvement design is to reduce settlement of the building and guarantee uniform (homogeneous) stiffness of the improved ground below the structure. The main advantages of the ground improvement compared to a heavy piling solution are:

- Minor soil disturbance with respect to soil stresses during the column installation compared to a bored piling.
- Faster installation times.
- No additional groundwater management during installation of columns is necessary.
- No rigid connection of the columns with the base slab, which is advantageous during seismic events.
- Simpler detailing with respect to the waterproofing system.
- Lower costs.

2 MATERIALS AND METHODS

The subject of the following part of the paper is the settlement prediction of the Nivy Station´s high-rise building via the finite element method. First, the soil conditions and constitutive models utilized and the procedures for determining their input values are identified. Then, the monitoring of the construction is briefly introduced. In the next chapter, the finite element model and the construction stages adopted are described. Finally, the results and an evaluation thereof are then presented.

2.1 Soil conditions, constitutive models and input parameters

Quaternary sediments (Q) consist of a layer of silty sands (SM) and poorly-graded gravels (GM). They only have a minor effect on the behaviour of a foundation system as their base is located above the foundation system. Tertiary sediments (T) are formed by a top layer of clayey sand (SC), mainly followed by clays with medium-to-high plasticity (CI, CH), interbedded with thin layers of clayey sand (CS) and sandy clay (CS). The original water level at Nivy Tower was 5.3 m below ground level. In terms of the index properties and the strength and stiffness parameters, only the Quaternary and Tertiary soils were distinguished; the hydraulic properties (the permeability coefficients for saturated soils) were determined separately for each of the partial layers based on permeability tests conducted during the triaxial testing.

The high-rise settlement was mostly influenced by Tertiary (Neogene) sediments. This section is therefore mainly focused on determination of the stiffness parameters for these soils. The Hardening Soil Model with Small Strain Stiffness (*Schanz et al., 1999*; *Benz et al., 2009*) was adopted and is denoted as HSS in this paper. The stiffness parameters were mainly derived from 19 1D compression tests, which were conducted on undisturbed samples for this project (*GES, 2014*). These tests were carried out as summarised in Tab. 1 and schematically shown in Fig. 1.

Tab. 1 *Procedure for conducting 1D compression tests*

Stage	Description	Initial stress	Final stress	Notation*
0	Loading to the original geostatic stress σ_{or}. Reconsolidation	0	σ'_{or}	-
1	Unloading from σ_{or} by the decrease in stress caused by excavation ($\Delta\sigma_{exc}$)	σ'_{or}	$\sigma'_{or} - \Delta\sigma'_{exc}$	E^{*}_{oed}
2	Reloading to the original geostatic stress	$\sigma'_{or} - \Delta\sigma'_{exc}$	σ'_{or}	E^{I}_{oed}
3	Loading from to the value of the expected foundation pressure from the upper structure ($\Delta\sigma_{max}$)	σ'_{or}	$\sigma'_{or} + \Delta\sigma'_{max}$	E^{II}_{oed}
4	Unloading back to the original geostatic stress	$\sigma'_{or} + \Delta\sigma'_{max}$	σ'_{or}	E^{**}_{oed}

** Notation of 1D compression modulus derived from the current stage. These moduli are in fact secant moduli between the initial and final stress state.*

Neogene sediments in the location of Bratislava are overconsolidated with an estimated overburden erosion thickness varying between 81 m and 272 m (*Galiková, 2018*). Assuming the effective unit weight $\gamma' = 20 - 9.8 = 10.2$ kN/m^3, this leads to values of pre-overburden pressure *(POP)* between 826 and 2774 kPa. This means that even with the lower bound of *POP*, the vertical pre-consolidation stress would not be exceeded during the high-rise construction. In term of the HSS model, all the 1D compression moduli in Tab. 2 might be referred to as the unloading-reloading moduli (E^{ur}_{oed}). However, significant differences were noted, especially between the values of E^{II}_{oed} and E^{*}_{oed} . Lower values of E^{II}_{oed} might be caused by the occurrence of elastoplastic deformations in the overconsolidated region as the void ratio gradually approaches the normal consolidation line (NCL) with an increasing stress level (*Nakai, 2012*). Furthermore, all the values measured are in fact secant moduli evaluated for different lengths of stress intervals (the stress interval was more than twice as long for E^{II}_{oed} compared to E^{*}_{oed}). Finally, the soil stiffness during the initial loading (E^{II}_{oed}) is sensitive to soil disturbances due to the sampling and preparation of the samples.

This effect has been studied by various authors. *Gilbert (1992)* performed a detailed review of the effects of sample disturbances on laboratory-measured soil properties. In the case of overconsolidated soils, these effects led to a decrease in the amount of stress required to compress the soil at a given void ratio. *Lim et al. (2018)* reported a significant reduction in the oedometric modulus observed in an overconsolidated range due to a sample disturbance.

Fully elastic behaviour during the unloading-reloading process is assumed in the HSS model. Furthermore, a tangent oedometric modulus is considered in the constitutive model. Therefore, the purely elastic unloading moduli and , unbiased by the development of the plastic strains and derived in a relatively narrow stress range, are further considered in the calibration of the input parameters. For the sake of simplicity, both moduli are referred to as in the following text. *Schmertmann (1953)*, in his graphic procedure, also used the slope of the unloading-reloading line to adjust (reconstruct) the virgin compression curve in the stress range between the current overburden pressure and the effective preconsolidation pressure. A regression analysis was then performed, and the reference stiffness value and the power exponent were determined assuming the stress – stiffness dependence according to the equation below. The approximation using this equation and the measured data points are shown in Fig. 2.

$$E_{oed,ur} = E^{ref}_{oed,ur}\left(\frac{c'\cos\varphi' - \sigma'_1\sin\varphi'}{c'\cos\varphi' + p^{ref}\sin\varphi'}\right)^{m} \quad (1)$$

Finally, the 1D reference compression moduli was converted into the Young´s modulus (Eq. 2), assuming elastic behaviour during the unloading where is the Poisson ratio in the unloading-reloading regime:

$$E^{ref}_{ur} = \frac{E^{ref}_{oed,ur}(1+\nu'_{ur})(1-2\nu'_{ur})}{(1-\nu'_{ur})} \quad (2)$$

The index, stiffness and strength are summarised in Tab. 3; the saturated permeabilities for the individual layers are stated in Tab. 4. The reference shear modulus at a very small strain G^{ref}_0 and the threshold shear strain governing the material model response in the very small-to-small strain range were not determined by the laboratory tests. They were estimated as follows: $G_0=3G_{ur}$, which might be considered as a conservative estimate, and $\gamma_{0.7}=1e^{-4}$.

Tab. 2 *Index, stiffness, and strength parameters*

Soil Group	γ_{unsat}	γ_{nsat}	E^{ref}_{50}	E^{ref}_{oed}	E^{ref}_{eur}	E^{ref}_{0}	m	c'	φ'	ψ	POP
	[kN/m^3]	[kN/m^3]	[MPa]				[-]	[kPa]	[°]	[°]	[kPa]
Quaternary	20.0	20.5	20.0	20.0	60.0	-	0.9	5	35	5	0
Tertiary	20.5	20.8	21.6	17.3	68.7	85.8	0.77	12.7	26.7	0	1000

Tab. 3 *Saturated permeabilities for the individual layers*

Soils, layers		k_{sat} [m/s]
Quaternary sediments		
Silty sand, clay with intermediate plasticity	SM, CI	1.2e^{-7}
Poorly-graded gravel	GP	1.0e^{-4}
Neogene sediments		
Sandy clay	SC	2.8e^{-6}
Clay sand	CS	2.1e^{-7}
Clay with intermediate to high plasticity	CH, CI	3.2e^{-8}

2.2 Monitoring the construction

The construction of the high-rise building was continuously monitored. Geodetical levelling (GL) was used to track settle-

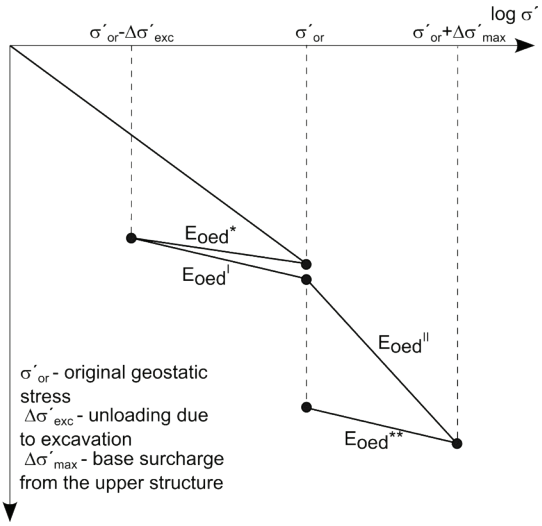

Fig. 1 *Schematic course of the laboratory test*

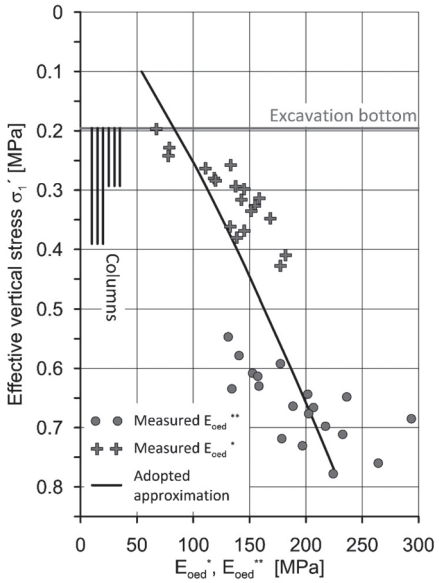

Fig. 2 *Measured compression moduli during unloading and their approximation*

ment of the structure. The results from 6 measured points (GL 1 to 6) were used in this study. Additionally, 4 sliding micrometres (SM I to IV) were installed beneath the foundation slab. The positions of the individual sensors are shown in Fig. 3.

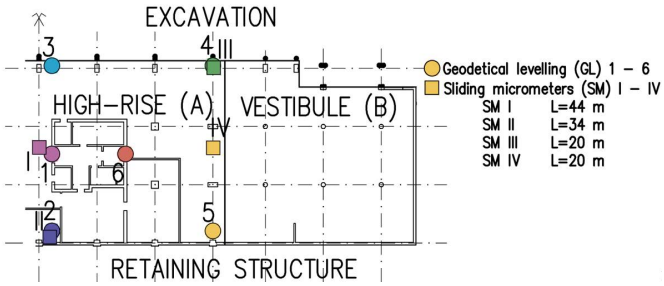

Fig. 3 *Position of the individual sensors*

3 COMPUTATIONAL MODEL

The building analysed consists of two parts. Part A is a high-rise with 32 aboveground and 2 underground floors with a total height of 125 m; part B is a vestibule with 4 aboveground floors and 2 underground floors. The schematic ground plan and a cross-section are shown in Figs. 4 and 5, respectively.

As the high-rise is symmetrical, only half of the construction was considered in the 3D finite element model. This has led to a significant reduction in the number of elements and thus the calculation time. It must be noted that the symmetry is not complete because the vestibule is only situated on one side of the high-rise. This simplification was considered acceptable as the surcharge pressure from the vestibule is significantly smaller compared to the high-rise. The FE model was prepared using Plaxis 3D 2023 software.

The upper structure was not modelled directly; instead, it was replaced by a set of point loads (columns), line loads (walls), and surface loads (a stiffening core). The construction of new floors was simulated by increasing these loads.

The foundation base is situated approximately 14 m below the original ground. The excavation was supported by a combination of two systems: a) a soil nail wall with a height of three meters and two levels of nails, b) a diaphragm wall stabilised by two levels of prestressed ground anchors. As the behaviour of the retaining system has only a minor influence on the high-rise foundation, it was simplified in the following way: the diaphragm wall was considered from the original ground and the soil nailing was omitted; two levels of soil nails were replaced by one level of ground anchors; and the individual anchors were modelled by zero prescribed displacement in the horizontal direction.

The raft foundations for the high-rise (Part A) and the lobby (Part B) have thicknesses of 2.3 m and 0.4 m, respectively. Both were modelled by isotropic plate elements. The raft foundation under the high-rise was supported with jet grouted columns. The columns were 9 and 18 m long with a designed diameter of 2 m, and they were constructed in a rectangular pattern at distances of 3.5 and 2.6 m. The jet-grouted columns were modelled using the embedded pile concept (*Sadek and Sahrour, 2004*). These are beam elements with embedded zero-thickness interface elements to model the pile-soil interaction along a shaft and on a pile base. Additional virtual nodes were generated inside the soil elements in the locations of the nodes of the beam element. The main advantage of the embedded pile concept is a reduction of the computational time; i.e., it is not necessary to use volumetric finite elements for discretization of the individual piles. The input parameter for these embedded beam elements were as follows: γ_c=21.5 kN/m^3 and E_c = 2 GPa; the ultimate skin friction was calculated from the strength parameters of the surrounding soil and the acting radial stress. A 10 % shear strength reduction of the concrete-soil interface compared to the soil-soil interface was considered (R_{inter} = 0.9). Overviews of the numerical model in its final stage, structural elements, and the loads replacing the upper structure are shown in Figs. 6 and 7, respectively. The finite element mesh consists of 41,730 10-noded tetrahedral elements.

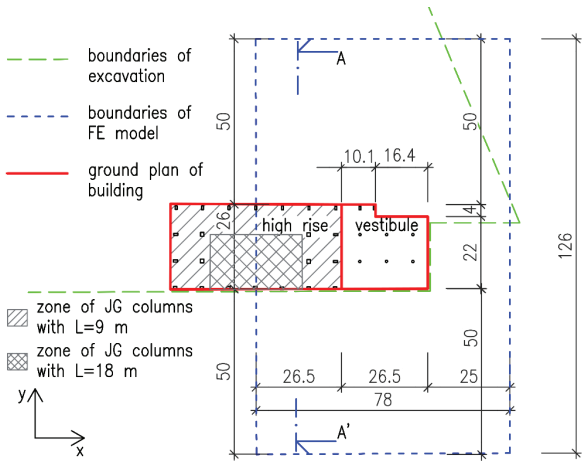

Fig. 4 *Schematic ground plan and FE model boundaries*

The high-rise construction was divided into 14 stages. Stage Nos. 1 – 3 (excavation, construction of the jet grouted columns, and foundation slab) were considered as drained. Steady state seepage conditions were assumed with the ground

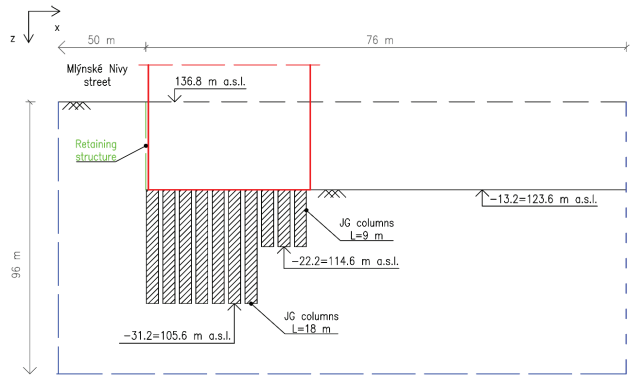

Fig. 5 *Schematic cross section A-A´ and FE model boundaries*

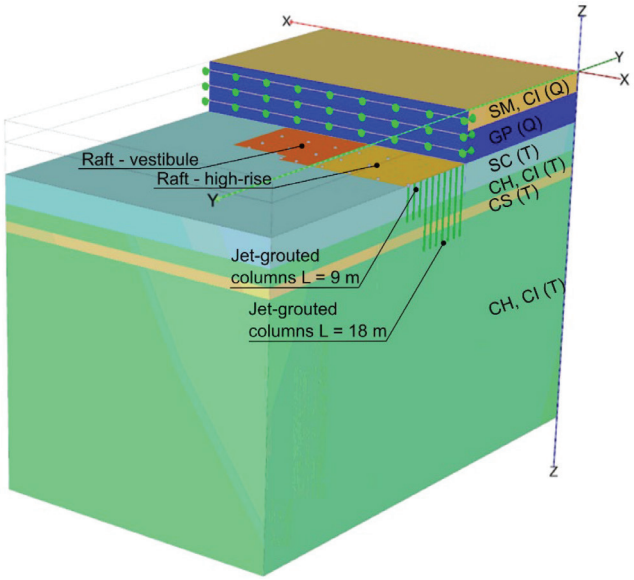

Fig. 6 *3D FE model with structural elements and soil conditions described*

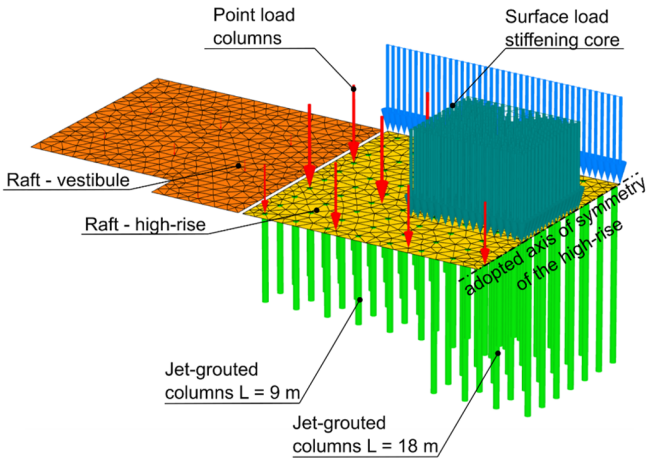

Fig. 7 *Structural elements of foundation and their discretization*

water level 0.5 m below the excavation bottom. In the next phases simulating the construction of the upper structure, the primary consolidation was enabled. In terms of the groundwater flow conditions, the vertical boundary in the axis of the symmetry of the high-rise and at the deepest horizontal boundary was considered as closed with a zero Darcy flux across the boundary.

4 RESULTS OF THE ANALYSIS

The predicted and measured time dependencies of the settlements for the 6 points analysed are shown in Fig. 8. The isosurfaces of the vertical displacements for Stage No. 11 after completion of all the upper floors are shown in Fig. 9. The duration of the time interval analysed was 973 days. As expected, the settlements increased in the direction from the vestibule to the center of the tower. In the direction of the shorter side, the settlements are smaller close to the retaining wall (Point Nos. 2 and 5) and higher on the opposite side of the slab (Point Nos. 3 and 4). The possible reasons for these differential settlements are:

Tab. 4 *Construction stages*

ID	Stage	Calculation type	Duration [day]	Share of total applied load* [%]
0	Initial conditions	K0 conditions	-	-
1	Excavation	Plastic drained	-	-
2	Construction of jet grouted columns		-	-
3	Construction of foundation slab		-	-
4	2 floors constructed	Consolidation	77	6.9
5	5 floors constructed		56	17.3
6	7 floors constructed, lobby		38	24.2
7	8 floors constructed		20	27.7
8	14 floors constructed		63	48.4
9	20 floors constructed		90	60.0
10	26 floors constructed		49	71.8
11	34 floors constructed		130	83.5
12	External cladding of structure		129	94.2
13	Completion of construction, consolidation		321	100

* from the upper structure

- Different overburdens next to the slab edge (excavated and retained area), causing various stiffnesses in the subsoil (stress-dependent stiffness).
- Possible soil loosening during the execution of bored piles in the adjacent area of the excavation pit (along the slab edge - Point Nos. 3 and 4).
- Effect of asymmetrical loading in combination with the varying JG column lengths below the slab.

The FE computations have predicted the overall behaviour with a reasonable degree of accuracy. The differences between the measured and predicted values at the end of the final loading stage (the last available measurement) varies between 3.4 % (Point No. 4) and 19.9 % (Point No. 2).

The results from the sliding micrometers are plotted in Fig. 10 for three construction stages: Stage No. 8 (14 floors constructed), Stage No. 11 (34 floors constructed) and Stage No. 12 (construction of the external cladding). The end of Stage No. 12 corresponds to the last measurement conducted via the sliding micrometers. The results are normalized with respect to the maximum value measured at this construction stage for a given micrometer. The computational results are processed in the same way. Micrometer Nos. I (L=44 m) and II (L=34 m) are located near the longer JG columns. The remaining two Micrometer Nos. III and IV with lengths of 20 m were constructed between the shorter JG columns. The results from Micrometer No. I are not discussed here as the plausibility of the measurements is questionable. The computed profiles in the positions of Micrometer Nos. III and IV sufficiently match with the measurements. Larger differences were observed for Micrometer No. II. The measured profile is similar to the numerical prediction up to a depth of approximately 22 m. Below this point, however, the calculations and measurements begin to differ.

Two additional computations were performed to analyse the efficiency of the selected foundation system:

- Study A: the column lengths were unified at 18 m (shorter columns with a length of 9 m were extended).
- Study B: No columns were considered; the foundation system only consists of the foundation slab.

The predicted vertical displacements are normalized with respect to the original solution and are shown in Fig. 11a (Stage No. 8: 14 floors constructed) and in Fig. 11b (Stage No. 11: 34 floors constructed). The extension of the columns led to a further settlement reduction of 7 % to 32 %. A higher effect was achieved in the area near the excavated part in which the shorter columns were located in the original solution. When only considering the foundation slab without any columns, a significant increase in the settlement (41% to 84 %) was obtained.

5 CONCLUSIONS

The foundation system consisting of the base slab and ground improvement using jet grouted columns proved to be a suitable solution for the foundation of Nivy Tower in Bratislava, Slovakia. The scope of the site investigation, including tests on undisturbed samples, allowed for a direct determination of some of the input parameters such as the unloading-reloading stiffness. However, the parameters governing the soil stiffness in the very small-to-small strain range had to be estimated. The impact of the unloading-reloading stiffness is substantial in this project, as the foundation pressure did not exceed the greatest vertical stress achieved in the past due to overconsolidation. The extensive construction monitoring, including the geodetical levelling and sliding micrometers,

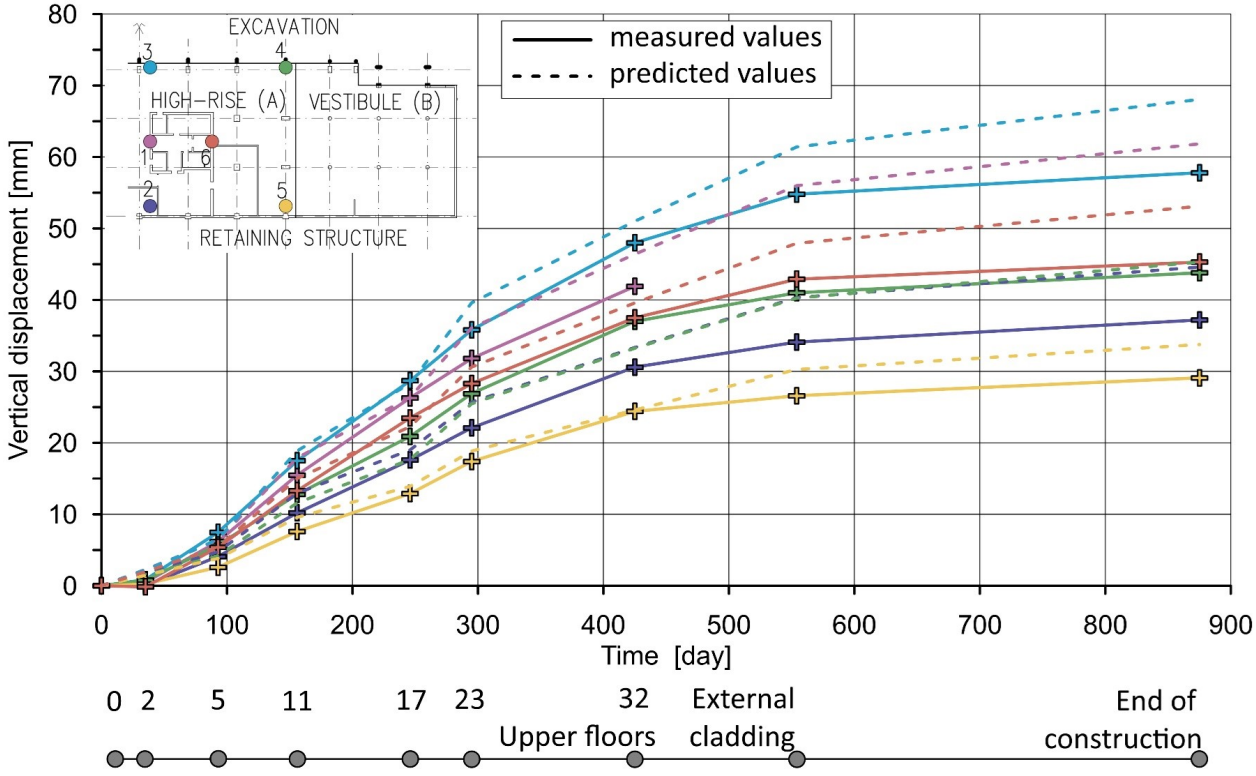

Fig. 8 *Measured and predicted settlements in different positions of the high-rise*

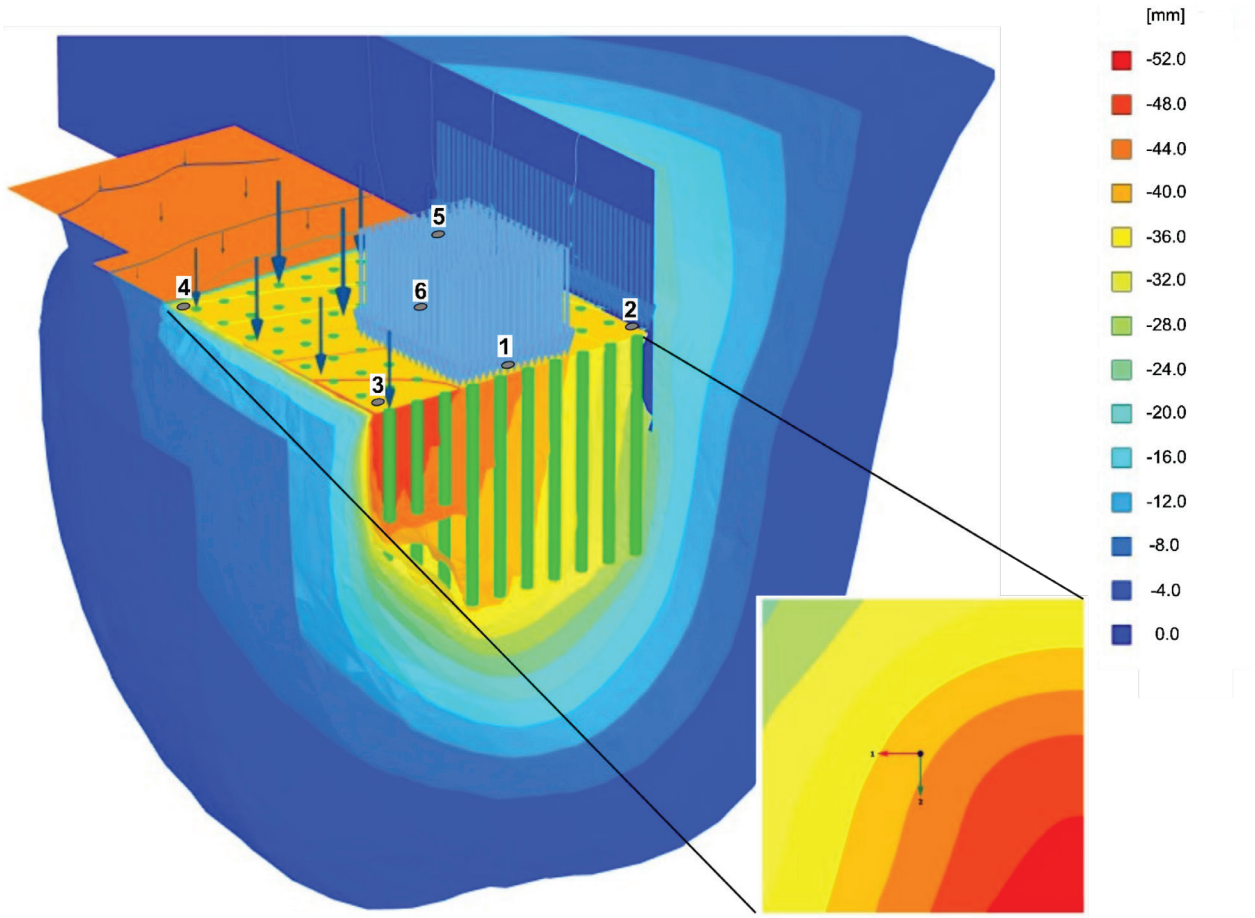

Fig. 9 *Isosurfaces of the vertical displacements at the end of Loading Stage No. 11 (after completion of all the upper floors)*

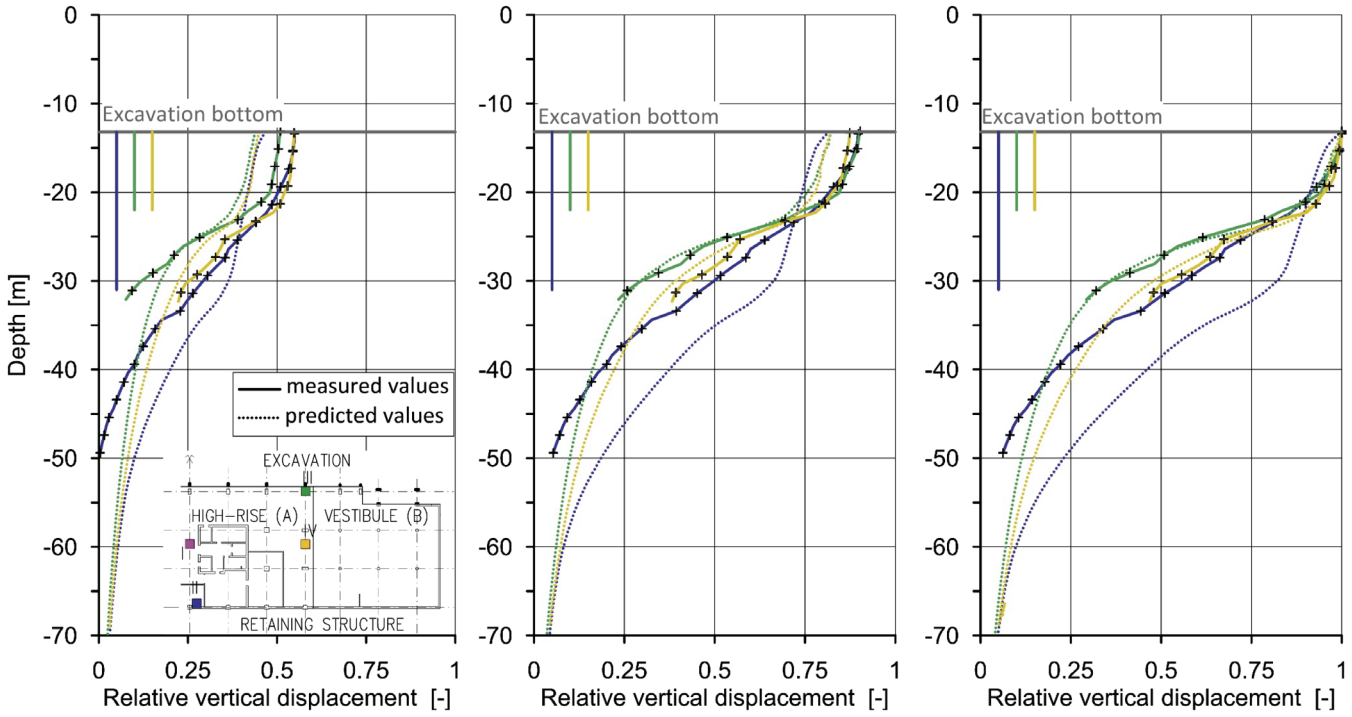

a) Stage No. 8 (14 floors constructed) *b) Stage No. 11 (34 floors constructed)* *c) Stage No. 12 (external cladding)*

Fig. 10 *Vertical displacement profiles measured by sliding micrometers and predicted by the FE model*

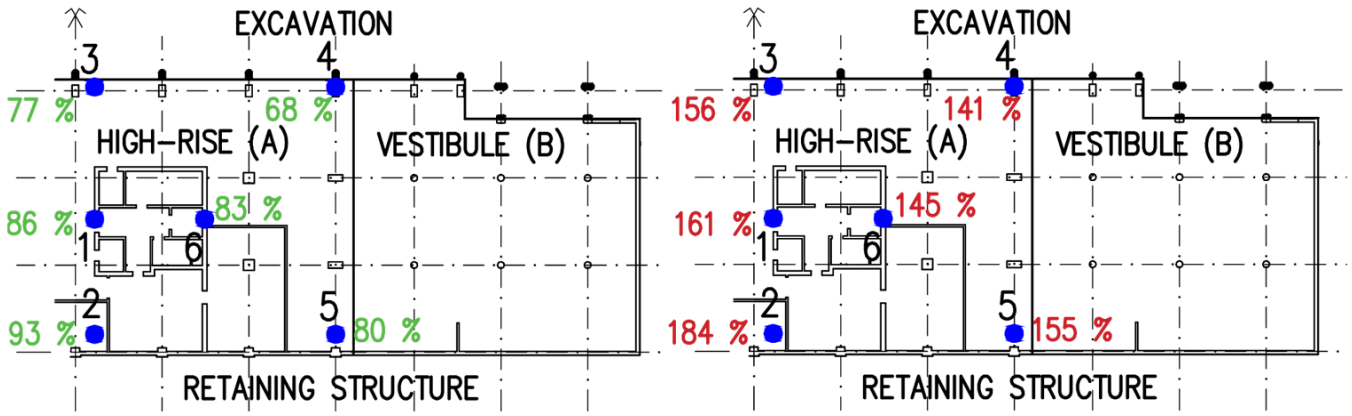

a) Study A – unified length of pile 18 m *b) Study B – no columns, only foundation slab*

Fig. 11 *Change in settlements relative to the original solution*

allowed for a detailed assessment of the accuracy of the computations performed. The finite element model correctly predicted the spatial course of the settlements, which increased in the longitudinal direction towards the high-rise´s centre of gravity and in a transverse direction towards the adjacent excavation. The maximum predicted settlement was 68 mm. The differences compared to the geodetic measurements ranged from 3.4 % to 19.9% in the last construction stage.

REFERENCES

Benz, T., Vermeer, P. A., & Schwab, R. (2009). A small-strain overlay model. *International journal for numerical and analytical methods in geomechanics*, **33(1)**, 25-44.

Galliková, Z. (2018). Experimental Analysis of Over-Consolidation in Subsoil in Bratislava, Slovakia. *Proceedings of China-Europe Conference on Geotechnical Engineering*, **1**, 514-518.

Ganal, A., & Reul, O. (2023). Back analysis of long-term measurements of a high-rise building founded on a raft foundation in overconsolidated clay. In *Proceedings of 10th European Conference on Numerical Methods in Geotechnical Engineering (NUMGE), London*.

GES ltd. (2014). Exploration works in Bratislava, Twin City North. Geotechnical test of soils (in Slovak).

Gilbert, P.A. (1992) Effect of sampling disturbance on laboratory-measured soilproperties. Department of the Army, Corps of Engineers, MiscellaneousPaper GL-92-35, Washington DC, USA.

Katzenbach, R., Schmitt, A. (2004). High-rise buildings in Germany soil-structure interaction of deep foundations.

Lambe, T. W. (1973). Predictions in soil engineering. *Géotechnique*, **23(2)**, 151-202.

Lim, G. T., Pineda, J., Boukpeti, N., Carraro, J. A. H., & Fourie, A. (2019). Effects of sampling disturbance in geotechnical design. *Canadian Geotechnical Journal*, ***56*(2)**, 275-289.

Nakai, T. (2012). Constitutive modeling of geomaterials: principles and applications. CRC Press.

Poulos, H. G. (2023). Analysis of foundation settlement interaction among multiple high-rise buildings. *Geotechnical and Geological Engineering*, *41*(5), 2815-2831.

Sales, M. M., Small, J. C., & Poulos, H. G. (2010). Compensated piled rafts in clayey soils: behaviour, measurements, and predictions. *Canadian Geotechnical Journal*, *47*(3), 327-345.

Sadek, M., & Shahrour, I. (2004). A three dimensional embedded beam element for reinforced geomaterials. *International journal for numerical and analytical methods in geomechanics*, ***28*(9)**, 931-946.

Schanz, T., Vermeer, P. A., & Bonnier, P. G. (1999). The hardening soil model: formulation and verification. *Beyond 2000 in computational geotechnics*, **1**, 281-296.

Schmertmann, J. H. (1953). Estimating the true consolidation behavior of clayfrom laboratory test results. *Proceedings of the American Society of Civil Engineers*, **79**: 1–26.

Topolnicki, M. (2019). Ground Improvement Instead of Piling – Effective Design Solutions for Heavily Loaded Structures.